Supplementary Information

Thermal and electrochemical interface compatibility of a hydroborate solid electrolyte with 3 V-class cathodes for all-solid-state sodium batteries

Ryo Asakura,[1,2] Léo Duchêne,[1] Seyedhosein Payandeh,[1] Daniel Rentsch,[3] Hans Hagemann,[2] Corsin Battaglia[1], and Arndt Remhof[1†]

[1] *Laboratory Materials for Energy Conversion, Empa, Swiss Federal Laboratories for Materials Science and Technology, 8600 Dübendorf, Switzerland*

[2] *Département de Chimie-Physique, Université de Genève, 1211 Geneva 4, Switzerland*

[3] *Laboratory for Functional Polymers, Empa, Swiss Federal Laboratories for Materials Science and Technology, 8600 Dübendorf, Switzerland*

[†] e-mail: arndt.remhof@empa.ch

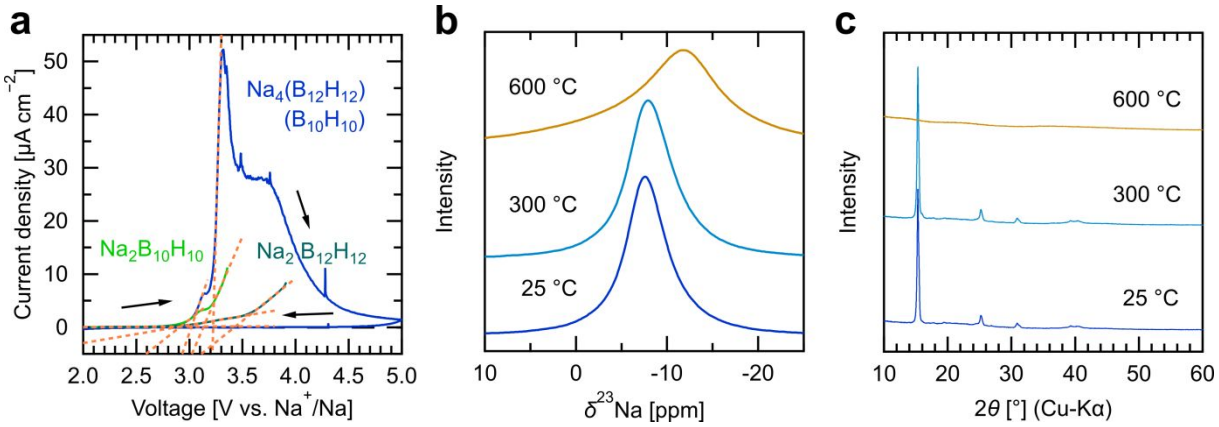

Fig. S1 (a) Full voltammograms of $Na_2B_{12}H_{12}$ (dark green) (Asakura, R. et al. *Energy Environ. Sci.* **2020**, *13* (12), 5048–5058), $Na_2B_{10}H_{10}$ (light green), and $Na_4(B_{12}H_{12})(B_{10}H_{10})$ (blue) (Asakura, R. et al. *ACS Appl. Energy Mater.* **2019**, *2* (9), 6924–6930) in Pt/SE-carbon/SE/Na cells (SE:carbon = 75:25 in weight) at a scan rate of 10 μV s^{-1} at 60 °C. (b) ^{23}Na MAS solid-state NMR spectra and (c) XRD patterns of $Na_4(B_{12}H_{12})(B_{10}H_{10})$ at 25 °C and after heating at 300 °C and 600 °C for >1 h under vacuum.

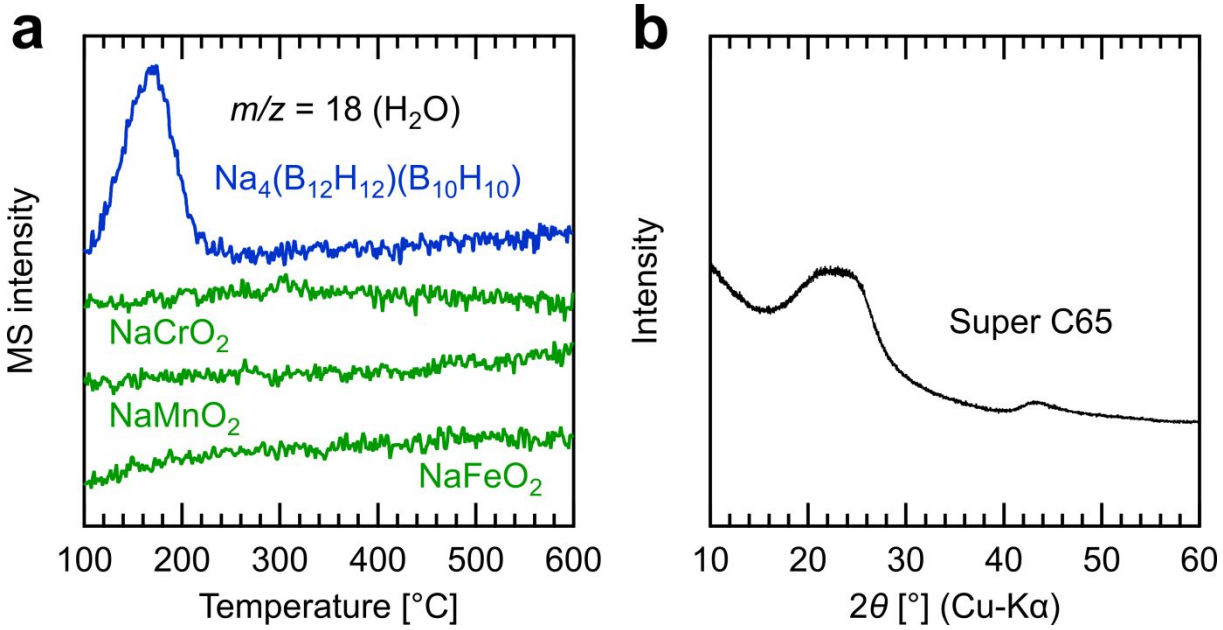

Fig. S2 (a) MS data ($m/z = 18$) of $NaCrO_2$, $NaMnO_2$, and $NaFeO_2$ at a heating rate of 5 K min^{-1}, plotted with $Na_4(B_{12}H_{12})(B_{10}H_{10})$ for comparison. (b) XRD pattern of the conductive carbon Super C65 at 25 °C in a borosilicate glass capillary.

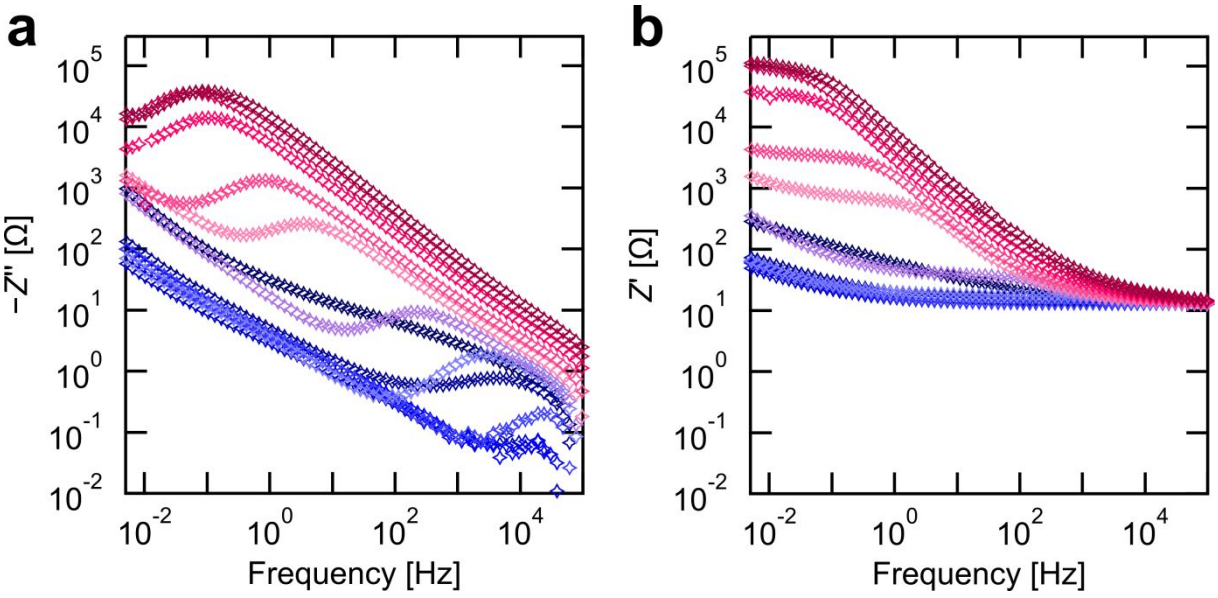

Fig. S3 (a) Imaginary part and (b) real part of the impedance spectra recorded after the constant voltage step at each upper cut-off voltage from 2.8 V to 3.9 V vs. Na^+/Na during the first charge of a $NaCrO_2|Na_4(B_{12}H_{12})(B_{10}H_{10})|Na$ all-solid-state cell at 60 °C. Each color represents the corresponding upper cut-off voltage shown in Fig. 3a.

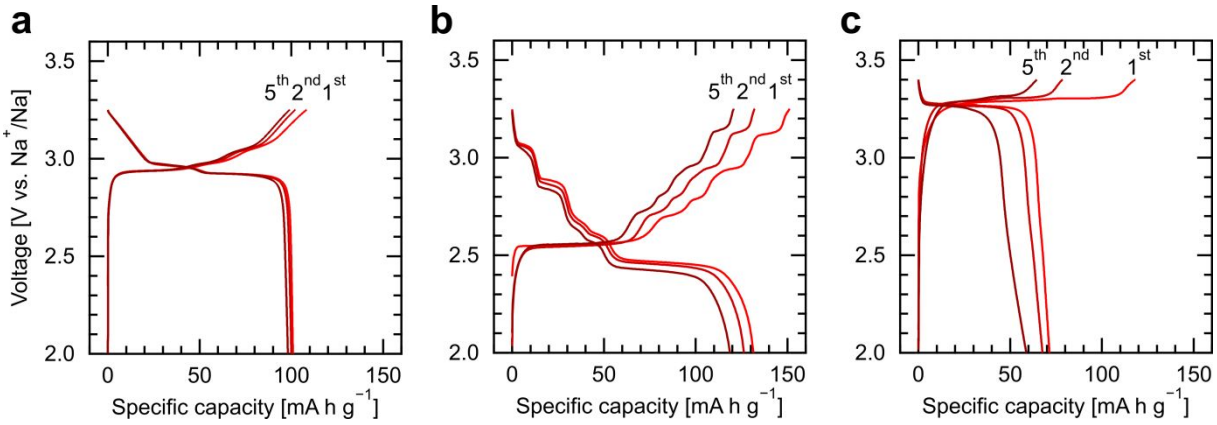

Fig. S4 Galvanostatic charge–discharge curves of $NaTMO_2|Na_4(B_{12}H_{12})(B_{10}H_{10})|Na$ all-solid-state cells with (a) $NaCrO_2$, (b) $NaMnO_2$, and (c) $NaFeO_2$, cycled between 2.00 V and 3.25 V (for $NaCrO_2$ and $NaMnO_2$) or 3.40 V (for $NaFeO_2$) vs. Na^+/Na at C/20 at 60 °C. The higher upper cut-off voltage was used for $NaFeO_2$ to reach its Fe^{3+}/Fe^{4+} redox potential.

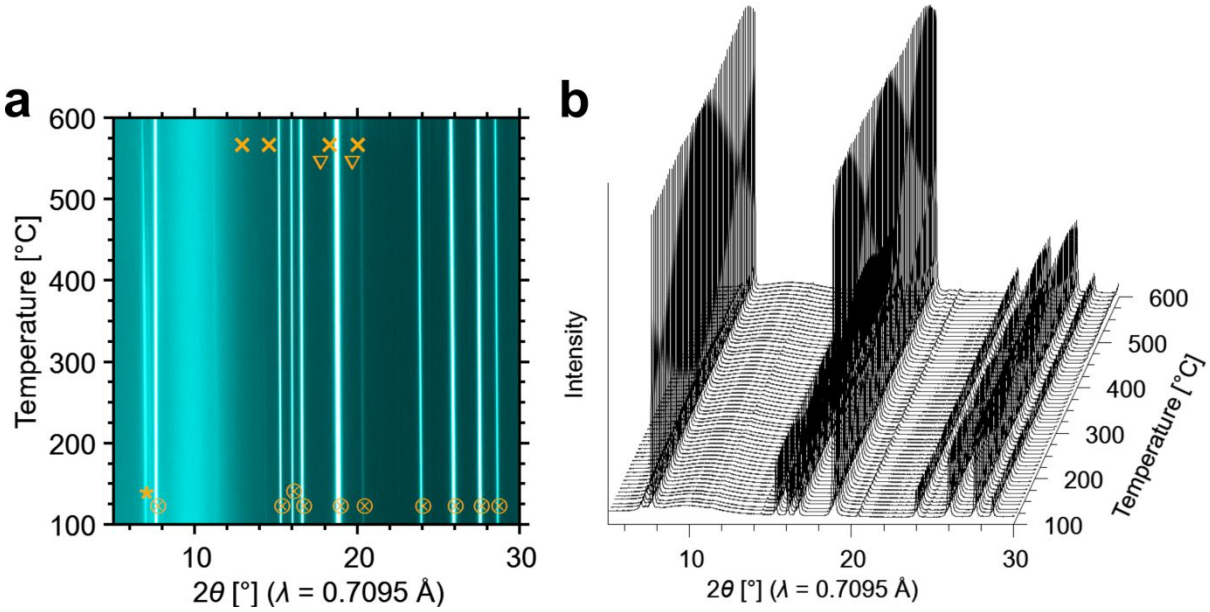

Fig. S5 (a, b) Temperature-dependent synchrotron XRD patterns of the $NaCrO_2$ cathode composite ($NaCrO_2$:$Na_4(B_{12}H_{12})(B_{10}H_{10})$:carbon = 70:20:10 in weight) at a heating rate of 20 °C min^{-1}. Each symbol corresponds to the phase observed in Fig. 2c.

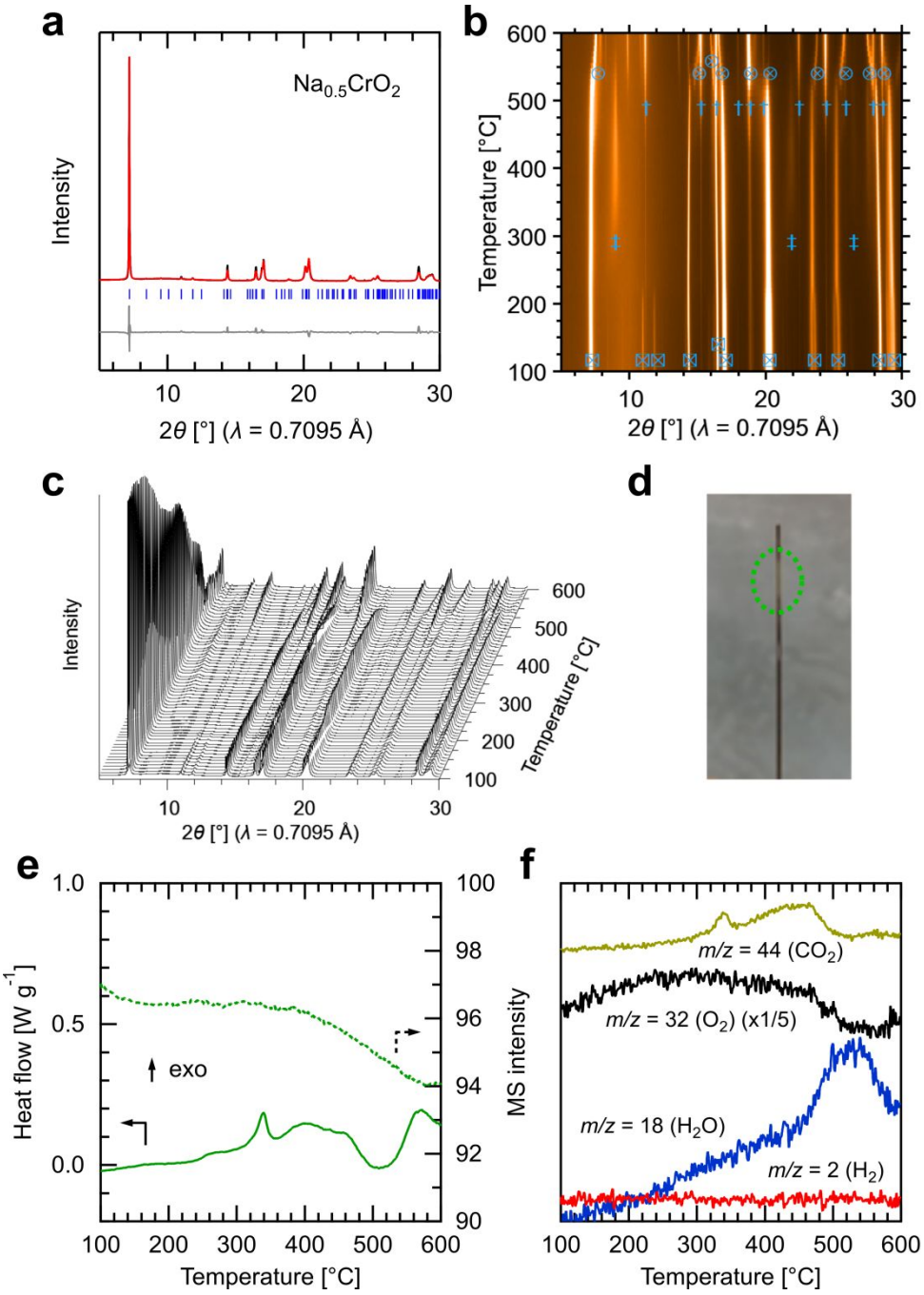

Fig. S6 (a) Synchrotron XRD pattern and Rietveld refinement of $Na_{0.5}CrO_2$ (R_{wp} = 8.43 %, χ^2 = 5.49) at 30 °C. (b, c) Temperature-dependent synchrotron XRD patterns of $Na_{0.5}CrO_2$ at a heating rate of 20 °C min^{-1}. (d) Capillary image of $Na_{0.5}CrO_2$ after the temperature-dependent synchrotron XRD measurements. The green circle depicts a color change to green in the heated sample region, indicating the formation of Cr_2O_3 and $NaCrO_2$. Each symbol corresponds to the phase observed in Fig. 4c. (e) DSC data (left axis) and TG (right axis) of $Na_{0.5}CrO_2$ recorded at a heating rate of 5 °C min^{-1}. (f) MS data of $Na_{0.5}CrO_2$.

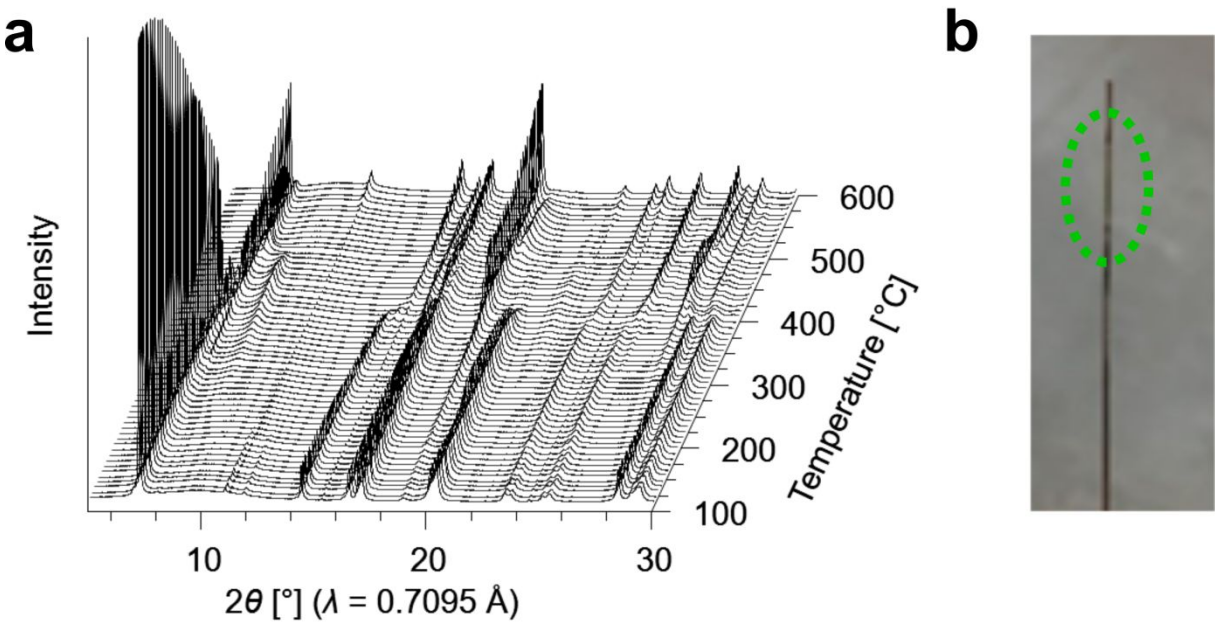

Fig. S7 (a) Temperature-dependent synchrotron XRD patterns of the $Na_{0.5}CrO_2$ cathode composite recorded at a heating rate of 20 °C min^{-1}. (b) Capillary image of the cathode composite after the temperature-dependent synchrotron XRD measurements. The green circle depicts a color change to green in the heated sample region, indicating the formation of Cr_2O_3 and $NaCrO_2$.